Random Access Preamble Sequence Design in High-Speed Scenario

Ziyuan Qiu[1(✉)], Sen Wang[2], Qixing Wang[2], Wenxi He[3], and Hang Long[1]

[1] Wireless Signal Processing and Network Lab, Key Laboratory of Universal Wireless Communication, Ministry of Education, Beijing University of Posts and Telecommunications, Beijing, China
qiuziyuan@bupt.edu.cn
[2] China Mobile Research Institute, Beijing, China
[3] Purple Mountain Laboratories, Nanjing, China

Abstract. Random access preamble sequences are sent from the user equipment (UE) to gNodeB though Physical Random Access Channel to access to the network. In high-speed scenarios, the performance of random access based on Zadoff-Chu sequences degrades due to the Doppler frequency offset which breaks the sub-carrier orthogonality. In this paper, a random access preamble sequence with linear change in phase is proposed based on the analysis of the influence of frequency offset on the correlation results of random access preamble sequence. The method of decreasing the peak-to-average power ratio of time domain sequence and the random access preamble sequence design compatible with orthogonal time-frequency space technology are proposed. The false detection rate and the timing error distribution are evaluated. The simulation results show that the proposed designs of random access preamble sequence are insensitive to frequency offset, and the detection performance and timing performance are almost unaffected by frequency offset.

Keywords: Random access · Doppler shift · OTFS

1 Introduction

The random access procedure is very important in realizing user equipment (UE) access to the network and uplink timing synchronization, in which UE sends a random access preamble to gNodeB (gNB) through Physical Random Access Channel (PRACH), and the gNB determines whether any UE accesses to the network and which UE accesses to the network by detecting the random access preamble sequence in the received signal based on peak energy and position of sequence correlation [1]. In 5G new radio (NR) system, random access preambles are generated based on the Zadoff-Chu (ZC) sequences. The good correlation of the ZC sequence avoids the problems of access conflict and inter-user interference when multiple UEs access [2, 3].

The Doppler frequency offset caused by the rapid movement of the UE will destroy the good correlation of the ZC sequence, thus affecting the random access performance.

F. Gao et al. (Eds.): ChinaCom 2022, LNICST 500, pp. 71–83, 2023.
https://doi.org/10.1007/978-3-031-34790-0_6

For the problem of random access in high-speed scenarios, Refs. [4] and [5] analyzed that the frequency offset would lead to the leakage of the peak energy of sequence correlation, resulting in multiple pseudo-peaks. Refs. [6] and [7] proposed a multi-window combined detection method at the receiver to overcome the problem of leakage of the peak energy, but its detection performance in high-speed scenarios will still deteriorate. Refs. [8] and [9] proposed frequency offset estimation methods based on PRACH, and then detect the random access preamble after frequency offset compensation, but it can only estimate the frequency offset in a certain range, and it is only suitable for a single frequency offset scenario.

According to the influence of frequency offset on peak energy and position of correlation, this paper designs an anti-frequency offset random access preamble sequence. On this basis, a method to solve the problem of large Peak-to-Average Power Ratio (PAPR) of time domain sequence is given. Considering the compatibility with multi-carrier modulation technology in 6G, this paper also proposes the design of anti-frequency offset random access sequences based on Orthogonal Time and Frequency Space (OTFS). The sequences proposed in this paper can meet the demand for the number of available sequences in the cell, and the demand for random access preamble detection and timing performance with the traditional single window detection method.

The rest of this paper is organized as follows. Section 2 describes the system model. Section 3 analyzes the influence of frequency offset on peak position and energy of correlation result. Section 4 puts forward an anti-frequency offset random access preamble sequence design and a method to decrease the PAPR, and Sect. 5 gives the design of random access preamble sequence based on OTFS. Section 6 presents the simulation results followed by the conclusion in Sect. 7.

Notations: $|\cdot|$ denotes the absolute value, $\langle\cdot\rangle$ represents rounding up, and $(\cdot)^*$ denotes the conjugate.

2 System Model

The 5G standard specifies [10] that the random access preamble sequences are generated from ZC sequences and different preambles are obtained by cyclic shift to meet the requirements of cell reuse. The rules for generating random access preamble sequences defined in 3GPP 38.211 protocol [10] can be denoted as

$$\begin{aligned} x_u(n) &= \mathrm{e}^{-j\frac{\pi un(n+1)}{L_{\mathrm{RA}}}}, n = 0, 1, ..., L_{\mathrm{RA}} - 1 \\ x_{u,v}(n) &= x_u[(n + C_v) \bmod L_{\mathrm{RA}}] \end{aligned} \tag{1}$$

where u is the physical root sequence number, L_{RA} refers to the length of ZC sequence, C_v is the cyclic shift, mod refers to Modulo operation. $x_{u,v}(n)$ is the random access preamble sequence generated by cyclic-shifting the root sequence $x_u(n)$.

Figure 1 shows the procedure of PRACH transmitter and receiver in the 5G system. $Y(m)$ is the frequency domain expression of $x_{u,v}(n)$.The time domain sequence $x_t(p)$ is obtained by $Y(m)$ with sub-carrier mapping and Inverse Fast Fourier Transform (IFFT), and then adds Cyclic Prefix (CP) to get random access transmission signal.

The gNB removes CP of received random access signal and then obtains the time domain sequence $x_r(p)$ denoted as

$$x_r(p) = Hx_t(p)e^{j\frac{2\pi\Delta f}{N_{FFT}\Delta f_{RA}}p} + q(p)\, p = 0, 1, \cdots, N_{FFT} - 1 \tag{2}$$

where H is the Line of Sight (LOS) channel gain, Δf denotes the Doppler frequency offset, N_{FFT} refers to the size of Fast Fourier Transform (FFT), Δf_{RA} is sub-carrier interval, and $q(p)$ refers to the noise [11]. Then $x_r(p)$ is transformed into the frequency domain sequence $Y_r(m)$ by FFT and sub-carrier de-mapping. The root sequence $Y_{root}(m)$ is the frequency domain expression of $x_u(n)$. Using the method of frequency domain correlation detection, $Y_r(m)$ and $Y_{root}(m)$ are conjugated multiplied to get $Y_c(m)$, and then the time domain correlation result is obtained through Inverse Discrete Fourier Transform (IDFT). Next, receiver implements preamble detection and timing estimation according to the energy and position of the peak of the time domain correlation result.

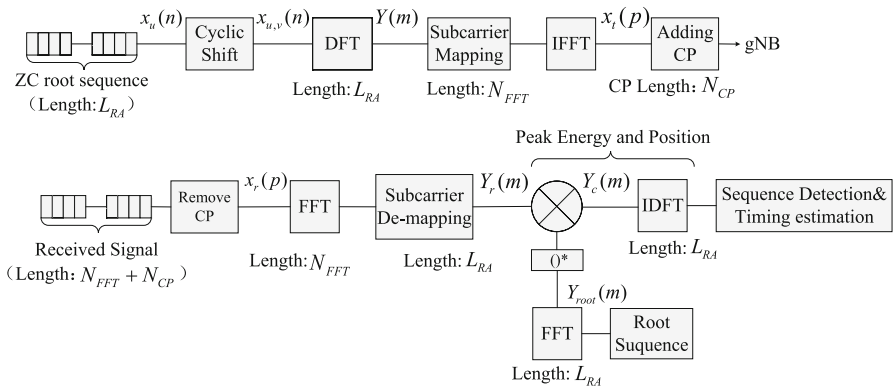

Fig. 1. System Model

3 Influence of Frequency Offset on Correlation Receiver

In high-speed scenarios, the frequency offset leads to the leakage of the peak energy of the correlation result of ZC sequence, which will reduce the detection performance and timing accuracy.

Reference [12] analyzes the influence of frequency offset on the correlation result of general sequence in the frequency domain. Without considering the noise, the result of the frequency domain correlation result at the receiver is simplified as

$$Y_c(m) \approx |K(0)|Y_{c,pre}(m) + Y_{c,interf}(m)\, m = 0, 1, \ldots, L_{RA} - 1 \tag{3}$$

where L_{RA} is the sequence length. Set

$$\begin{aligned} Y_{c,pre}(m) &= HY(m)Y_{root}(m)^* \\ Y_{c,interf}(m) &= \sum_{k=1}^{L_{RA}-1} Y_{c,interf,k}(m) - \sum_{k=-(L_{RA}-1)}^{-1} Y_{c,interf,k}(m) \\ Y_{c,interf,k}(m) &= H|K(k)|Y_{1,k}(m)Y_{root}(m)^* \\ Y_{1,k}(m) &= \begin{cases} Y(m+k), \max(0,\ -k) \le m \le \min(L_{RA}-1, L_{RA}-1-k) \\ 0, \text{else} \end{cases} \\ k &= -(L_{RA}-1), -(L_{RA}-2), \cdots, -1, 1, 2, \cdots, L_{RA}-1 \end{aligned} \tag{4}$$

where H is the LOS channel gain, $Y_{c,pre}(m)$ refers to the frequency domain correlation result without frequency offset, while $Y_c(m)$ has an additional interference $Y_{c,interf}(m)$ consisting of $Y_{c,interf,k}(m)$ compared to it. $Y_{c,interf,k}(m)$ is the interference to the current sub-carrier by a sub-carrier with distance k from the current sub-carrier, and $K(k)$ is the coefficient of this interference, denotes as

$$\begin{aligned} K(k) &= \begin{cases} \frac{1}{N}e^{j\theta_0}\left|\frac{\sin\left(\frac{\Delta f}{\Delta f^{\mathrm{RA}}}\pi\right)}{\sin\left(\frac{\Delta f+k\Delta f^{\mathrm{RA}}}{N_{FFT}\Delta f^{\mathrm{RA}}}\pi\right)}\right| e^{j\left(\frac{-k}{N_{FFT}}\right)\pi}, 0 \le k \le N_{FFT}-1 \\ \frac{1}{N}e^{j\theta_0}\left|\frac{\sin\left(\frac{\Delta f}{\Delta f^{\mathrm{RA}}}\pi\right)}{\sin\left(\frac{\Delta f+k\Delta f^{\mathrm{RA}}}{N_{FFT}\Delta f^{\mathrm{RA}}}\pi\right)}\right| e^{j\left(\frac{-k}{N_{seq}}+1\right)\pi}, -(N_{FFT}-1) \le k < 0 \end{cases} \\ \theta_0 &= \frac{(N_{FFT}-1)\Delta f\pi}{N_{FFT}\Delta f^{\mathrm{RA}}} \end{aligned} \tag{5}$$

where N_{FFT} is the FFT size. The absolute value of $K(k)$ decreases to close to 0 as the absolute value of k increases.

The time domain correlation result can be denoted as

$$x_c(p) \approx |K(0)|x_{c,pre}(p) + x_{c,interf}(p)\ p = 0, 1, \ldots, L_{RA}-1 \tag{6}$$

where $x_c(p)$, $x_{c,pre}(p)$ and $x_{c,interf}(p)$ are the time domain expressions corresponding to the terms in Eq. (3), and

$$x_{c,interf}(p) = \sum_{k=1}^{L_{RA}-1} x_{c,interf,k}(p) - \sum_{k=-(L_{RA}-1)}^{-1} x_{c,interf,k}(p) \tag{7}$$

$x_{c,interf,k}(p)$ is the time domain expression of $Y_{c,interf,k}(m)$. Set p_c, $p_{c,pre}$, $p_{c,interf}$ and $p_{c,interf,k}$ to be the peak positions of $x_c(p)$, $x_{c,pre}(p)$, $x_{c,interf}(p)$ and $x_{c,interf,k}(p)$ respectively. According to (6) and (7), when $p_{c,interf,k} = p_{c,pre}$, the frequency offset has no effect on the peak position of the correlation result, but the peak energy is slightly affected; when $p_{c,interf,k} \neq p_{c,pre}$, the peak energy and position of the correlation result are greatly affected by the frequency offset.

Applying the ZC sequence to the above analysis, results in an offset $kd_u\langle N_{FFT}/L_{RA}\rangle$ in $p_{c,interf,k}$ compared to $p_{c,pre}$ [12]. du is defined as

$$d_u = \begin{cases} q, \ 0 \le q < L_{RA}/2 \\ L_{RA} - q, \ else \end{cases} \\ (uq) \bmod L_{RA} = 1 \tag{8}$$

Figure 2 shows the peak position relationships between $x_{c,pre}(p)$ and $x_{c,interf,k}(p)$ with different values of d_u. When $d_u = 1$, both the peak energy and position of ZC sequence have affected by frequency offset. When $d_u \neq 1$, the offset of the peak position of the interference leads to multiple pseudo-peaks instead of only one main peak in the correlation result. In addition, as the frequency offset increases, the energy of the main peak decreases and the energy of the pseudo-peak increases. When the frequency offset is equal to the sub-carrier interval, the energy will be concentrated on the pseudo-peak, and the energy of the main peak is too weak to be detected, so the detection and timing performance of the random access seriously decreases.

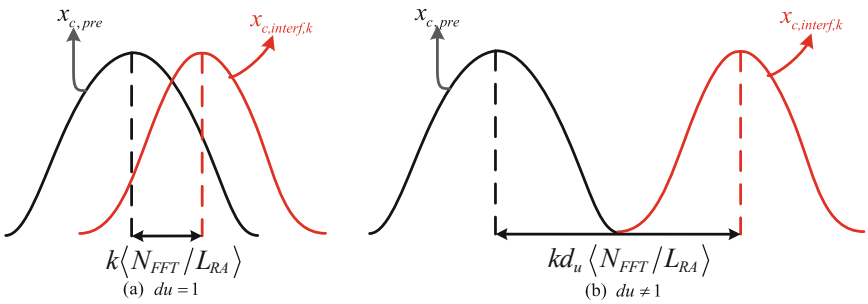

Fig. 2. Peak position relationship between $x_{c,pre}(p)$ and $x_{c,interf,k}(p)$ of ZC sequence

4 The Design of Random Access Preamble Sequence

4.1 Anti-frequency Offset Random Access Preamble Sequence

Based on the analysis of the influence of frequency offset on the correlation result in Sect. 3, a sequence with a constant module value of 1 and linear change in phase are proposed as the random access preamble sequence in frequency domain, which is defined as

$$\mathrm{X}(m) = e^{jm\left(\theta_h + \frac{2\pi C_v}{L_{RA}}\right)} \ m = 0, 1, \cdots, L_{RA} - 1 \tag{9}$$

where C_v is cyclic shift, and θ_h refers to phase slope, that is, the phase difference between two points in the sequence when the cyclic shift is 0, $\theta_h \in [0, 2\pi)$.

The module value of the frequency domain sequence is constant, and the corresponding time domain sequence has good autocorrelation characteristic. Applying $\mathrm{X}(m)$ to

Eq. (4), the result of time domain correlation calculation without frequency offset can be denoted as

$$x_{c,pre}(p) = \sum_{L_{RA}} e^{jm\left(\frac{2\pi(C_v+p)}{L_{RA}}\right)} \quad p = 1, 2, \ldots, L_{RA} - 1 \tag{10}$$

and the kth interference can be denoted as

$$x_{c,interf,k}(p) = H|K(k)| \sum_{L_{RA}} e^{jk\theta_h} \cdot e^{jm\left(\frac{2\pi(C_v+p)}{L_{RA}}\right)} \quad p = 1, 2, \ldots, L_{RA} - 1 \tag{11}$$

where $\max(0, -k) \leq m \leq \min(L_{RA} - 1, L_{RA} - 1 - k)$. It is easy to get that the peak position of the kth interference and the correlation without frequency offset are the same from (10) and (11), that is $p_{c,interf,k} = p_{c,pre}$. Figure 3 shows the peak position relationships between $x_{c,pre}(p)$ and $x_{c,interf,k}(p)$ of X sequence. According to Sect. 3, X(m) avoid influence of frequency offset on peak position of correlation result effectively.

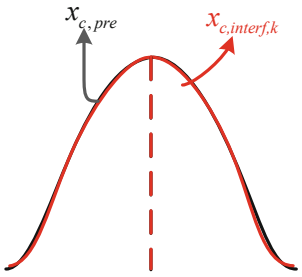

Fig. 3. Peak position relationships between $x_{c,pre}(p)$ and $x_{c,interf,k}(p)$ of X sequence

According to (7), the interference of the correlation result at receiver is essentially the sum of all kth Interference. In fact, it is not enough to achieve $p_{c,interf,k} = p_{c,pre}$. It is necessary to further determine whether $p_{c,interf} = p_{c,pre}$ is satisfied. According to (7) and (11), the interference of the correlation result at receiver can be denoted as

$$x_{c,interf}(p) = H \sum_{m=0}^{L_{RA}-1} e^{j\left(\frac{2\pi m(C_v+p)}{L_{RA}}\right)} \cdot \left[\sum_{k=1}^{L_{RA}-m-1} |K(k)|e^{jk\theta_h} - \sum_{k=-m}^{-1} |K(k)|e^{jk\theta_h} \right] \tag{12}$$

From Eq. (12), it can be found that after summing all the kth interferences the peak position may change due to θ_h and the characteristic of $K(k)$. Let

$$G(m) = \sum_{k=1}^{L_{RA}-m-1} |K(k)|e^{jk\theta_h} - \sum_{k=-m}^{-1} |K(k)|e^{jk\theta_h} \tag{13}$$

When the absolute value and phase of $G(m)$ are constant, $p_{c,interf} = p_{c,pre}$. According to Eq. (5), $|K(k)|$ takes its maximum value at $k = 0$, the larger $|k|$, the smaller $|K(k)|$,

and $|K(k)| = |K(k - L_{RA})|, k = 1, 2, \ldots, L_{RA} - 1$. On this basis, the absolute value and phase of $G(m)$ are constant when $\theta_h = \pi$. As $|\theta_h - \pi|$ increases, the absolute value and phase of $G(m)$ will vary more significantly with m, and vary greatest with m when $\theta_h = 0$. Consider θ_h as close to π as possible, but not close to 0.

4.2 Anti-frequency Offset Random Access Preamble Sequence with Low PAPR

The time domain expression of $\mathrm{X}(m)$ can be denoted as

$$x(p) = \frac{1}{\sqrt{L_{RA}}} \frac{\sin\left(\frac{L_{RA}}{2}\right)}{\sin\left(\frac{\theta_h}{2} + \frac{(p+C_v)\pi}{L_{RA}}\right)} e^{j\left[\frac{(L_{RA}-1)\theta_h}{2} + \frac{(p+C_v)\pi}{L_{RA}}\right]} p = 0, 1, \ldots, L_{RA} - 1 \quad (14)$$

It can be obtained that the time domain sequence has a significant peak at $\left\langle \left| \theta_h L_{RA} \middle/ 2\pi \right| \right\rangle - C_v$ with a high PAPR. A high PAPR in the time domain sequence increases the demands on the linear power amplifiers of transmitter and receiver and reduces transmission efficiency. The linear change in phase of the $\mathrm{X}(m)$ makes it resistant to frequency offset, but also introduces the problem of large PAPR of the time domain sequence. Consider reducing the PAPR of the time domain sequence by appropriately reducing the linear characteristics of the sequence, while meeting the requirement of random access performance.

According to analysis in Sect. 3 $|K(k)|$ close to 0 when $|k|$ is large. It can be ignored whether $Y_{c,interf,k}(m)$ with large $|k|$ is affected by frequency offset, which is the frequency domain correlation result of sequence with cyclic shift k and root sequence. On the other hand, the sequence only needs to keep a linear change in phase over a certain length.

Thus, a spliced sequence of multiple X sequences is proposed. In order to achieve a balance between the anti-frequency offset and low PAPR characteristics, the length of each subsequence is set to be equal and the phase slope difference between adjacent subsequences is equal, with the phase slope distributed around π. The spliced sequence is defined as

$$Xa(m) = \begin{cases} e^{jm(\pi - b'\Delta\theta + \Delta\theta + \frac{2\pi C_v}{L_{RA}})}, m = 0, 1, \cdots, L_b - 1 \\ \cdots \\ e^{jm(\pi - \Delta\theta + \frac{2\pi C_v}{L_{RA}})}, m = (b'-2)L_b, (b'-2)L_b+1, \cdots, (b'-1)L_b - 1 \\ e^{jm(\pi + \frac{2\pi C_v}{L_{RA}})}, m = (b'-1)L_b, (b'-1)L_b+1, \cdots, b'L_b - 1 \\ \cdots \\ e^{jm(\pi + b\Delta\theta - b'\Delta\theta + \frac{2\pi C_v}{L_{RA}})}, m = (b-1)L_b, (b-1)L_b+1, \cdots, L_{RA} - 1 \end{cases} \quad (15)$$

where b is the number of subsequence, $b' = \langle b/2 \rangle$, $L_b = \langle L_{RA}/b \rangle$ refers to the length of subsequence, $\Delta\theta$ is the difference of phase slope between adjacent subsequences, C_v denotes the cyclic shift. The stronger the linearity of the sequence, the better characteristic of anti-frequency offset and the higher PAPR of the time domain sequence. Increasing

the number of subsequences or increasing the phase slope difference of adjacent subsequences weakens the sequence linearity, which will deteriorate the anti-frequency offset characteristic. Therefore, the number of subsequences and the phase slope difference need to be set according to different scenarios to control the phase linearity of the sequences.

5 The Design of Random Access Preamble Sequence Based on OTFS

The OTFS technology proposed for 6G enables highly reliable, high-speed data transmission in doubly-selective fading channel, which modulates data directly in the Delay-Doppler (DD) domain and extends over the time-frequency domain [13]. Consider designing a random access preamble sequence in the DD domain. Discrete signals in DD domain can be transformed into the time-frequency domain though an M-point FFT and an N-point IFFT on the columns and rows of a $M \times N$ DD domain signal matrix, respectively. Thus, define the random access preamble sequences in the DD domain as

$$\mathrm{Xo}[k,l] = \begin{cases} 1 & k = a, l = 0 \\ 0 & else \end{cases} \begin{cases} k = 0, 1, \ldots, M-1 \\ l = 0, 1, \ldots, N-1 \end{cases} \tag{16}$$

After IFFT, the signal of time-frequency domain can be denoted as

$$x[m,n] = \frac{1}{\sqrt{NM}} \sum_{l=0}^{N-1} \sum_{k=0}^{M-1} \mathrm{Xo}[k,l] \mathrm{e}^{j2\pi\left(\frac{nl}{N} - \frac{mk}{M}\right)} = \frac{1}{\sqrt{NM}} \mathrm{e}^{-j\frac{2\pi am}{M}} \begin{cases} m = 0, 1, \ldots, M-1 \\ n = 0, 1, \ldots, N-1 \end{cases} \tag{17}$$

It is obtained that the signal is linear change in phase in the frequency domain and can be regarded as an X sequence with $\theta_h + 2\pi C_v / M = -2\pi a / M$ in Sect. 4.1. The value of a is determined by the phase slope θ_h and the cyclic shift C_v.

Several 1s are placed at different locations in the delay domain as random access preamble sequences of different UEs for different UEs in the DD domain, and then the time-frequency domain signals are obtained though Inverse Symplectic Finite Fourier Transform (ISFFT). The sequences of different users are orthogonal in the time domain, which leads to multiple separated peaks in the time domain correlation results. Different UEs are identified based on the peak locations. The maximum number of UEs for random access that can be carried in an OTFS frame is determined by the length of the delay domain and the timing error tolerance of channel.

In addition, it can be found that the time-frequency domain signal includes N OFDM symbols based on Eq. (17). The receiver performs correlation on the N OFDM symbols respectively. The detection performance can be improved by combining the N correlation results in high-speed scenario.

6 Simulation Results and Analysis

In this section, the detection performance and timing performance of the proposed anti-frequency offset random access preamble sequence are simulated and evaluated in high-speed scenarios and compared with the performance of PRACH format 0 defined in

3GPP 38.211 protocol [10]. The simulations are carried out on Additive White Gaussian Noise (AWGN) channel and Tapped Delay Line-D (TDL-D) channel respectively and the antenna configuration and channel model are based on the 3GPP 38.104 protocol [14]. In the case of restricted type A for ZC sequence, the receiver in simulation adopts multiple-windows combined detection algorithm [6, 7], while in all other cases the conventional receiver with single-window detection algorithm is adopted [15]. For OTFS-based random access preamble sequence, only the correlation result of the first OFDM symbol received is used for detection and timing. Table 1 and Table 2 show the system simulation parameters and sequence design parameters respectively.

Table 1. System simulation parameters

Parameters	Values
Carrier Frequency	2.6 GHz
Bandwidth	40 MHz
Sub-carrier Interval	1.25 kHz
Antenna Configuration	1Tx, 2Rx
Delay Spread	TDL-D: 300 ns
Time Error Tolerance	AWGN: 1.04 μs TDL-D:2.55 μs

Table 2. Sequence Design parameters

Parameters	Values
PRACH format 0 (ZC sequence)	Unrestricted (0Hz), restricted type A (625 Hz\1340 Hz): $u = 40, C_v = 0$
Anti-frequency offset sequence (X sequence)	$C_v = 0, \theta_h = \pi / 2$
Low PAPR sequence (Xa sequence)	$M = 1024, d = 10, \Delta\theta = \pi / 20, C_v = 0$
OTFS-based sequence (Xo sequence)	$N = 12, M = 1024, a = 257, C_v = 0$

6.1 Detection Performance

This section evaluates the detection performance of different random access preamble sequence based on 3GPP 38.104 protocol [14], which specifies that the PRACH detection performance must meet the false alarm probability of no more than 0.1% and the false detection rate of less than 1%. While satisfying the false alarm probability, the signal-to-noise ratio (SNR) at the false detection rate of 1% is taken as the metric of detection performance.

From Fig. 4 and Fig. 5, the detection performance of X sequence on AWGN and TDL-D is almost unaffected by frequency offset, while the performance of Xa and Xo sequence is slightly degraded with increasing frequency offset. The performance degradation of Xa and Xo sequence at 1340 Hz is less than 0.5 dB compared to no frequency offset.

In addition, the sequence proposed in this paper has a significant performance gain over the ZC sequence. When the frequency offset is 1340 Hz, the performance gain of X, Xa and Xo sequence are 0.91 dB, 0.76 dB and 1.82 dB respectively compared to the ZC sequence on AWGN, and the performance gain are 1.28 dB, 1.02 dB and 2.35 dB on TDL-D. And the performance gain of 625 Hz will larger than that frequency offset of 1340 Hz. The reason is that when frequency offset is 625 Hz, i.e., half the sub-carrier interval, the energy of peak spreads more, the pseudo-peak in the correlation result is the almost same energy as the main peak, while at a frequency offset close to the sub-carrier interval (1340 Hz), the correlation results still only have a distinct peak, which leads to better detection performance at frequency offset of 1340 Hz than 625 Hz.

The Xo sequence has the same phase slope as the X sequence, and its sequence length is 1024, which is larger than the sequence length of the X sequence, resulting in its detection performance is slightly better than that of the X sequence. Combining the correlation of all OFDM symbols in receiver, the performance gain is approximately 8 dB compared to receiver using only the correlation of the first OFDM symbol.

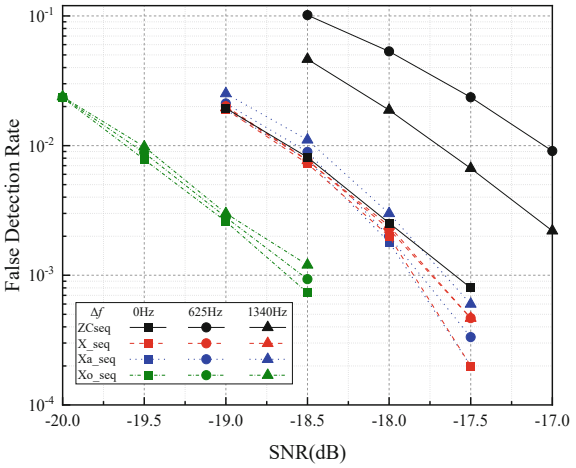

Fig. 4. Detection performance on AWGN

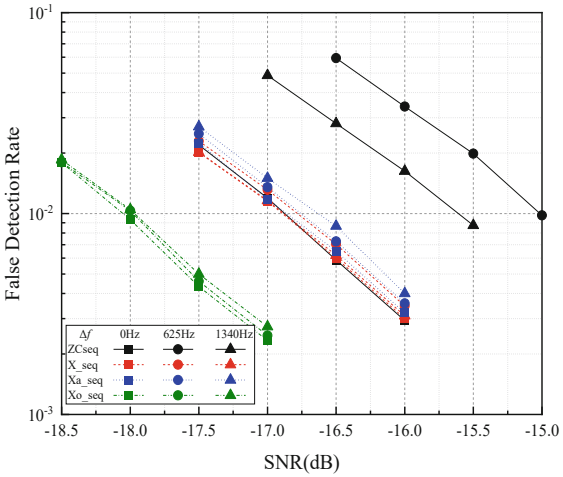

Fig. 5. Detection Performance on TDL-D

The PAPRs of the X and Xa sequences are evaluated in the simulations and are 187.8 and 6.2 respectively. Thus, the Xa sequence is achieving a large decrease in PAPR at the expense of slight anti-frequency offset characteristic.

6.2 Timing Performance

This section evaluates the timing performance of different random access preamble sequences based on the timing error distribution, the specific method is with the limitation of timing error tolerance, timing based on the peak position of the correlation results, the difference with the ideal peak position as the timing error, $\Delta t = 1 / \Delta f_{RA} \cdot N_{IFFT}$ as the unit of timing error, statistics to obtain the timing error Cumulative Distribution Function (CDF).

Figure 6 and Fig. 7 show the timing error distributions of the ZC, X and Xa sequences for SNR of −18 dB on AWGN and −16 dB on TDL-D, respectively. It can be found that the timing errors of the sequences on both channels are controlled within 13 Δt. With the influence of frequency offset, the timing performance of the ZC sequence based on the multiple-window combined detection algorithm slightly decreases, the timing error distribution of the X sequence is the same as when there is no frequency offset. The timing performance of the Xa sequence decreases due to frequency offset, and the larger the frequency offset, the larger the timing error. The reason is that the linear characteristic of the Xa sequence is weakened compared to the X sequence, and its anti-frequency offset characteristic is consequently weakened, resulting in a larger peak position offset. However, the timing error of Xa sequence is still controlled within 13 Δt, which is less than 16 Δt, the timing accuracy of PRACH in 5G NR system [16] and satisfies the requirement of PRACH timing performance.

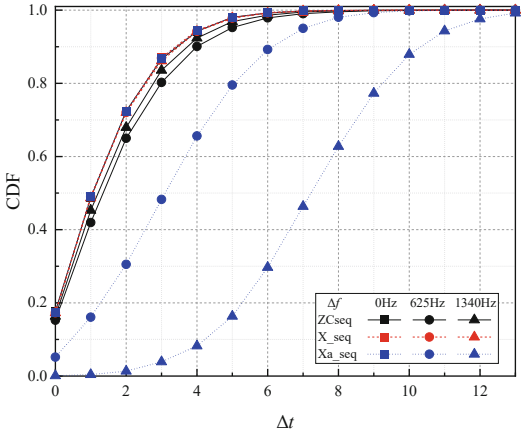

Fig. 6. Timing performance on AWGN

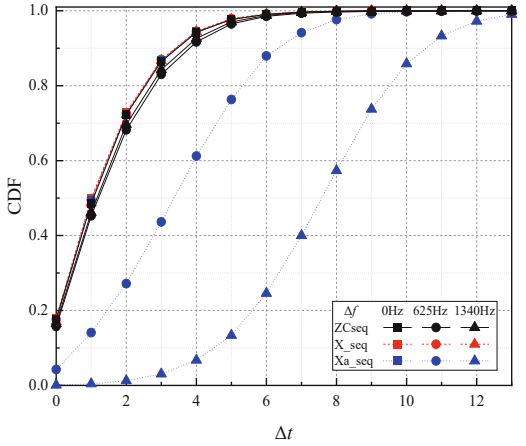

Fig. 7. Timing performance on TDL-D

7 Conclusion

This paper proposes a design of anti-frequency offset random access preamble sequence for high-speed scenarios, replacing the random access preamble sequence generated from the ZC sequence, avoiding the problem of frequency offset destroying the good correlation of the ZC sequence, which causes random access performance degradation. This paper also provides a method to reduce the time-domain PAPR of this sequence, as well as a sequence design method based on OTFS. According to the simulation results on AWGN and TDL-D channels, it is concluded that the proposed sequence is insensitive to frequency offset and can improve the detection performance and timing performance of random access in high-speed scenarios.

Acknowledgement. This work is supported by National Natural Science Foundation of China (No. 61931005) and Beijing University of Posts and Telecommunications-China Mobile Research Institute Joint Innovation Center.

References

1. Sanguinetti, L., Morelli, M., Marchetti, L.: A random access algorithm for LTE systems. Trans. Emerging Telecommun. Technol. **24**(1), 49–58 (2012)
2. Kim, J., Munir, D., Hasan, S., et al.: Enhancement of LTE RACH through extended random access process. Electron. Lett. **50**(19), 1399–1400 (2014)
3. Leyva-Mayorga, I., Tello-Oquendo, L., Pla, V., et al.: On the accurate performance evaluation of the LTE-A random access procedure and the access class barring scheme. IEEE Trans. Wireless Commun. **16**(12), 7785–7799 (2017)
4. Hua, M., Wang, M., Yang, W., et al.: Analysis of the frequency offset effect on random access signals. IEEE Trans. Commun. **61**(11), 4728–4740 (2013)
5. Thota, J., Aijaz, A.: On performance evaluation of random access enhancements for 5G uRLLC. In: 2019 IEEE Wireless Communications and Networking Conference (WCNC), pp. 1–7 (IEEE)
6. Huang, C., Ma, W., Luo, L.: Detection of random access preamble sequences in ultra high speed mobile environment. Syst. Eng. Electron. Technol. **40**(09), 2100–2105 (2018)
7. Min, T., Wen, W., Xu, Z.: High-speed mobile receiver algorithm in LTE system. Mobile Commun. **42**(6), 73–79 (2018)
8. Cao. A., Xiao, P., Tafazolli, R.: Frequency offset estimation based on PRACH preambles in LTE. In: 2014 11th International Symposium on Wireless Communications Systems, Barcelona, Spain, pp. 22–26 (2014)
9. Jun, W., Bao, G., Liu, S., et al.: Frequency offset estimation based on peak power ratio in LTE system. J. China Univers. Posts Telecommun. **2013**(6), 49–54 (2013)
10. 3GPP TS 38.211 V16.3.0. NR; Physical Channels and Modulation (2020)
11. Zhang, Y., Zhang, Z., Hu, X.: An improved preamble detection method for LTE PRACH based on Doppler frequency offset correction. In: Liu, X., Cheng, D., Jinfeng, L. (eds.) ChinaCom 2018. LNICST, vol. 262, pp. 573-582. Doi. Springer, Cham (2019). https://doi.org/10.1007/978-3-030-06161-6_56
12. He, W., Du, Y., Long, H.: Analysis of frequency offset effect on prach in 5g nr systems. In: 2019 14th International Conference on Communications and Networking in China (ChinaCom), Shanghai, China, pp. 679–692 (2019)
13. Long, H., Wang, S., Xu, L., et al.: OTFS technology research and prospect. Telecommun. Sci. **37**(09), 57–63 (2021)
14. 3GPP TS 38.104 V16.3.0. NR; Base Station (BS) Radio Transmission and Reception (2020)
15. Chen, Y., Wen, X., Zheng, W.: Random access algorithm of LTE TDD system based on frequency domain detection. In: 2009 Fifth International Conference on Semantics, Knowledge and Grid, pp. 346–350 (2009)
16. 3GPP TS 38.213 V16.3.0. NR; Physical layer procedures for control (2020)